

The coating of $n[\text{SiO}_{1.5}-(\text{CH}_2)_3(\text{NH}_2)]$ ultrathin layers on the surface of Fe_3O_4 nanoparticles and the analysis of their coating dynamics

P. ZAMORA IORDACHE*, V. ȘOMOĞHI, I. SAVU, N. PETREA, G. MITRU, R. PETRE, B. DIONEZIE^a, V. ORDEANU^b, L. KIM^c, L. MUTIAC^c

Scientific Research Center for NBC Defence and Ecology, 225, Olteniței, Bucharest, Romania

^aPolitehnica University of Bucharest – Biomaterials Research Center, 313, Spl. Independentei, Bucharest, Romania

^bMedico-Military Scientific Research Center, 37, C.A. Rosetti, Bucharest, Romania

^cUniversity of Bucharest, Department of Analytical Chemistry, 4-12, Regina Elisabeta Blvd., 030018 Bucharest, Romania

This paper presents the unitary and controlled synthesis of nanostructures of the type $\text{Fe}_3\text{O}_4-n[\text{SiO}_{1.5}-(\text{CH}_2)_3(\text{NH}_2)]-\text{S}_{n\theta}$ [Fe_3O_4 = magnetic core; $n[\text{SiO}_{1.5}-(\text{CH}_2)_3(\text{NH}_2)]$ = coating layer; $-\text{NH}_2$ = layer made up of groups which play an important part in biochemical interface; $\text{S}_{n\theta}$ = exterior layer of biochemical cross-linked molecules]. The purpose of obtaining these nanostructures is to fix $\text{Fe}_3\text{O}_4-n[\text{SiO}_{1.5}-(\text{CH}_2)_3(\text{NH}_2)]-\text{S}_{n\theta}$ on microorganism surface through covalent chemical bounds in order to determine them in magnetic field, as a function of the mass and volume of the microorganisms attached to the nanostructures. The nanocomposite materials with physical and chemical features induced in a controlled way in the basic physical structure in order to handle in a controlled manner the host structures, constitute a research field of current interest. The nanostructures we have drawn up are also important in fields connected to chemistry, such as: selective/unselective chemical separation, molecular macrocomplexes labeling, chemical/biological detection media and others.

(Received June 10, 2008; accepted June 30, 2008)

Keywords: Fe_3O_4 - SiO_2 - NH_2 core-shell nanoparticle, Superparamagnetic, Cross-linked molecule

1. Introduction

The detection of biological agents, of their metabolism products, of chemical and biological macrocomplexes with high toxicologic potential, constitutes a current problem whose solution has not been found yet. The difficulty of defining a theoretical and technological solution derives from the informational complexity of molecular organization at the level of macrocomplexes of the type bacterium, virus, toxin, etc. [1]. Another element which influences radically the correctness of the biochemical recognition, which has to be taken into account when one draws up new biological and chemical detection techniques and methods is the evolutionary character of microorganisms [2]. This makes defining the physical and chemical structures of microorganisms impossible in time, even if one starts from constitutional states initially known, as the microorganism evolution is given by the local nanoscopic physical and chemical conditions and by the inherent properties of the microorganism [3]. This structural indefiniteness can

favour or not the occurrence in time of random processes. The current techniques regarding the fast detection and identification of the previously mentioned bio structures are inefficient when a highly precise answer is required, in real time. The highly precise biological and chemical detection depends on a set of observables which should not depend on the local physical and chemical conditions [4]. For instance, the mass and volume of a microorganism may be regarded as invariable physical observables, characteristic for the relevant biological or chemical structure.

This paper presents the experimental data obtained as a result of the controlled syntheses of Fe_3O_4 nanoparticles and their coating in thin layers of $n[\text{SiO}_{1.5}-(\text{CH}_2)_3(\text{NH}_2)]$ [5] **C1**. On the C1 surface $-\text{NH}_2$ groups were implemented chemically and in a controlled manner. Their role is to facilitate the formation of covalent chemical bonds with a series of classes of biological and chemical cross-linked molecules which play an important role in the direct biochemical fixing (fig.1), of the ‘molecular spacer’ type (S) [6]. The objective of our research was to obtain

polystructured nanostructures having unitary physical and chemical properties, inserted in a controlled way, well delimited in point of placement inside the nanostructure and completely differentiable in initially known external physical conditions. The structure of the synthesized nanostructure is $\text{Fe}_3\text{O}_4\text{-n}[\text{SiO}_{1.5}\text{-(CH}_2\text{)}_3\text{(NH}_2\text{)}]\text{-S}_{\text{n}0}$ (C2). The control physical and chemical parameters inserted in C2 are chosen in relation with the type of process of biological and chemical detection and identification that has been settled. The insertion of these parameters was done in the phase of controlled chemical synthesis, in several stages, according to the data presented in this paper.

2. Experimental

2.1 Method

In order to implement the nanoparticles in the chemical synthesis stage, the following physical and chemical properties [7] were drawn up and placed in different space regions in the initial stage, as follows : a) the physical properties [8] (magnetic moment, Curie temperature, etc.) are generated by the Fe_3O_4 magnetic core situated in the central area of the nanostructure and whose dimensions are smaller than 30 nm (fig.1) b) the relevant chemical properties (the potential of biochemical fixing) are generated by the -NH-S groups [S = epoxide, aldehyde etc.] coated on the C1 surface [9].

The biological and chemical cross-linked molecules must have chemically active centres of the $\text{-S-S}_{\text{activated}}$ type and be placed within the nanostructure of the $\text{Fe}_3\text{O}_4\text{-n}[\text{SiO}_{1.5}\text{-(CH}_2\text{)}_3\text{(NH}_2\text{)}]\text{-[S-S}_{\text{activated}}\text{]}_{\text{n}0}$ type, so as the biochemical fixing should take place directly.

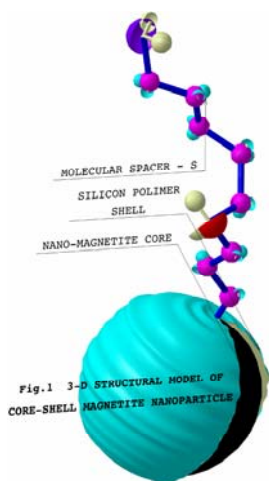


Fig. 1. 3-D Structural model of core-shell magnetite nanoparticle.

The C1 layer has the function of establishing a physico-chemical interface between the magnetite core, the molecular spacer and the chemically active centres responsible with the biological and chemical cross-linking. This interface is absolutely necessary from a practical perspective, as the magnetite has a low reactivity in comparison with the vast majority of relevant organic macrostructures [10, 11]. The thickness of the C1 layer, its specific surface, its hydrodynamic form and the superficial density of -NH-S groups, chemically induced on the C1 surface, influences significantly the C2 kinematics in the carrying fluid, the host medium of biochemical fixing and the biochemical fixing efficiency. Next we will present the way we obtained C2 and the theoretical modeling according to the experimental results of optimum fixing and magnetic discrimination of biostructures in fluids parameters.

2.2 The Fe_3O_4 nanoparticle synthesis

The Fe_3O_4 nanoparticle suspension was obtained through FeCl_3 coprecipitation (8,58g- Acros Organics) and FeCl_2 (23,275g - Acros Organics) in molar report $\text{Fe}^{2+}/\text{Fe}^{3+}=1:2$ [12]. The reaction volume was 1000 ml (FeCl_3 , FeCl_2 and distilled water), and the coprecipitation base was NH_3 (60 ml, 25% - Bucharest Reactive). Fe_3O_4 was obtained according to the chemical equation in (1):



Before initiating abruptly the coprecipitation reaction in the presence of NH_3 , the iron salts were weighed separately, dissolved in 10 ml of distilled water and supersonic stirred for 15 minutes at the frequency of 55KHz.

The time of initiating and growth of magnetite nanoparticles in the reaction medium was of 30 minutes, after the coprecipitation reaction took place [13,14]. During the entire initiating process and growth of Fe_3O_4 crystal, the rate of stirring with ultrasounds was of 55 KHz. The nanoparticle suspension was separated through magnetic decantation, using a magnet, and the pH of the

suspension reached the value of 7,5÷8 through successive magnetic washings and decantations.

2.3 The solubilisation of Fe_3O_4 nanoparticles in water

Before coating the Fe_3O_4 in SiO_2 , the nanoparticle suspension must be stabilized the coprecipitating reaction [15].

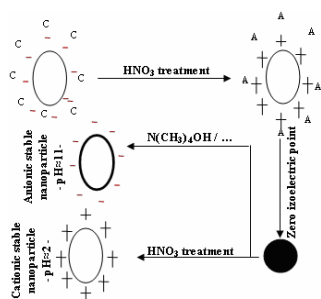


Fig. 2. Izoelectric stabilization diagram of Fe_3O_4 nanoparticles used in the presented syntheses and proposed for the first time by F. Tourinho [16]

C – cationic surfacted Fe_3O_4 nanoparticle
A – anionic surfacted Fe_3O_4 nanoparticle.

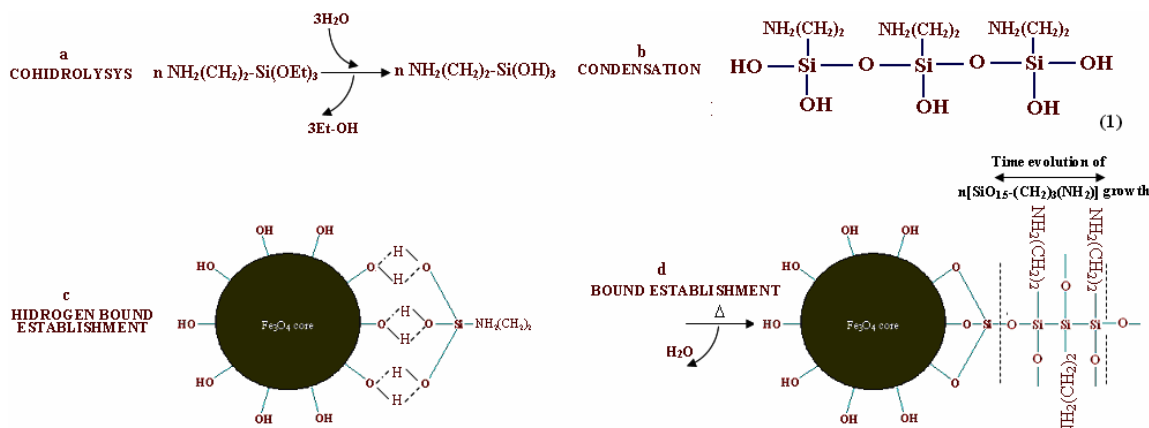


Fig. 3. Synthesis and $n[\text{SiO}_{1.5}-(\text{CH}_2)_3(\text{NH}_2)]$ coating of Fe_3O_4 nanoparticle.

The reaction volume was of 1000 ml, which consisted of 480ml absolute ethylic alcohol (Chimreactiv), 50 ml NH_3 -25%, ~4g Fe_3O_4 , the rest being completed with distilled water. The reaction lasted for 120minutes and 30 ml of sample were taken from 15 to 15 minutes in order to analyse the nanoparticles through transmission electronic microscopy (TEM) and scanning electronic microscopy (ESEM) [22]. The temperature of the reaction volume was of 60°C , and the stirring frequency through ultrasounds was of 55 KHz. The pH of the samples reached the value of 7,5-8 through distilled water washing.

For the study of C3 nanoparticle morphology we used the transmission electronic microscope Philips S208,

The stabilization was carried out by treating Fe_3O_4 with azotic acid (100ml, 2,3M) for 15 minutes, according to the chart in figure 2 [16].

As a result of the treatment with azotic acid a series of izoelectric stabilization nitrates emerged (especially NH_4NO_3), as well as a large quantity of $\text{Fe}(\text{NO}_3)_3$ resulted from the process of partial degradation of magnetite nanoparticles.

The disposal of the nitrates resulted in the izoelectric stabilization stage was carried out through distilled water washing and magnetic separation until the pH of the suspension reached the value of 7,5-8.

Supplementary, the Fe_3O_4 suspension underwent a treatment with sodium citrate tribasic dehydrate (100ml, 50 %, Merck) [17,18] for 15 minutes, in order to passivate [19] the synthesized nanoparticle surface through the superficial density diminishing of the electric charge distributed on the Fe_3O_4 surface.

2.4 The coating of Fe_3O_4 nanoparticles in $n[\text{SiO}_{1.5}-(\text{CH}_2)_3(\text{NH}_2)]$. To obtain Fe_3O_4 - $n[\text{SiO}_{1.5}-(\text{CH}_2)_3(\text{NH}_2)]$ (C3)

SiO_2 was deposited on the Fe_3O_4 surface through the cohydrolysis [20,21] of 14 ml (3-aminopropyl)-triethoxysilane - ($\text{C}_9\text{H}_{23}\text{NO}_3\text{Si}$, Merck), according to the following chemical reaction (1):

having the following working parameters: voltage acceleration 80 kV, spot 3, beam current 19 μA and olympus camera.

The compositional determination of C3 was carried out with the scanning electronic microscope ESEM Philips XL30, having the following working parameters: voltage acceleration 25kV, sample current 70 μA , analysis mode ESEM, X radiation analyzer EDAX.

The samples of analysed nanoparticles were magnetically refiltered before the analyses, in order to dispose of the residual magnetic clusters.

3. Results and discussion

Fig. 3 (a), (b), (c) represents pictures taken by the transmission electronic microscope Philips S208.

The C3 diameter is comprised in the interval 8-120 nm. This is a direct consequence of competitive processes of the following type: the quantity of the cohydrolysis agent, isoelectric stabilization, washing, stirring rate, the intensity of the filtering magnetic field, the duration of the magnetic filtering, etc..

From a morphologic perspective, the Fe_3O_4 nanoparticles have a spherical shape, and the rate of deviation from this shape is low. The C1 layer deposited on the nanoparticle surface has the same morphologic feature as the one of the support magnetite cores. The pictures we obtained are indicative of the fact that, besides the magnetite, C1 nanoparticles were formed.

Pure C1 nanoparticles are adjacent to Fe_3O_4 nanoparticles and their morphology and geometric size are similar to the ones of C3. Moreover, C3 and C1 are joined through buffer areas made up of silicon bridges. One has to notice the thickness of the silicon layer which is placed between the following values: P1 $d \in 40 \div 60 \text{ nm}$; P2 $d \in 40 \div 60 \text{ nm}$; P3 $d \in 10 \div 16 \text{ nm}$; P4 $d \in 70 \div 120 \text{ nm}$; P5 $d \in 10 \div 14 \text{ nm}$; P6 $d \in 30 \div 48 \text{ nm}$; P7 $d \in 11 \div 15 \text{ nm}$; P8 $d \in 8 \div 17 \text{ nm}$.

The tested conducted using the ESEM had as an objective the compositional determining of C3 in order to determine the optimum synthesis parameters [23] and the thickness variation of the C1 layer in time. Two different scans were conducted for each of the 8 tests (with and without carbon – support analysis medium). The content of Fe, Si, N and O is illustrated in tab.1, and the X radiation spectra specific to the analysed elements are illustrated in **fig.LabelA:F_iP_i fara C**, $i=1 \div 8$.

The Fe quantity remains constant during the process of magnetite coating, with the variance of the quantity of coated Si, N, O, alone. The variance of the intensity of spectral lines emitted by Fe is a consequence of the number of nanoparticles on which the electron beam is focussed. Besides the Fe, Si, N and O content noted in table no. 1 small quantities of Na, Al, Ca, Cl and K were also detected. These come from the reaction agents that

were used in the syntheses and from the stages of biochemical coating and activation.

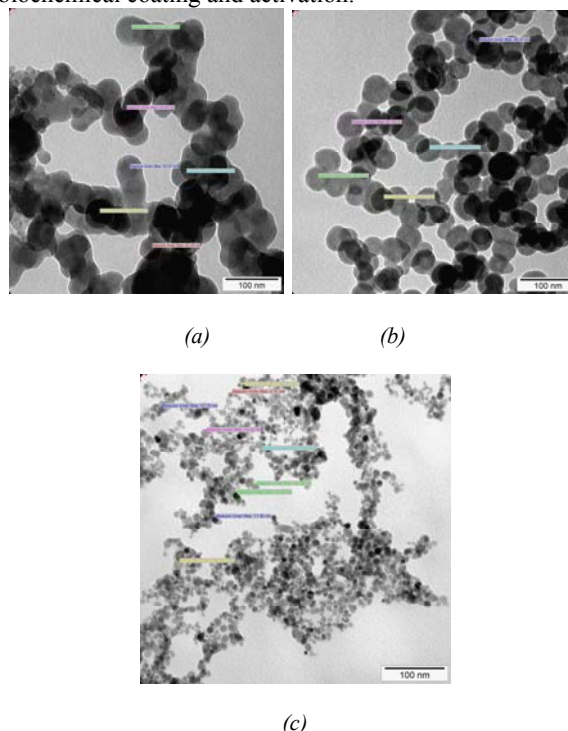


Fig. 3. (a) Picture TEM of C3, 15 minutes after the beginning of the reaction, direct magnification 180.000x; (b) Picture TEM of C3, 90 minutes after the beginning of the reaction, direct magnification 180.000x; (c) Picture TEM of C3, 120 minutes after the beginning of the reaction, direct magnification 180.000x.

In the characteristic X rays spectrum one can identify four lines that correspond to Fe. These are due of a different emission of characteristic X rays by Fe_2O_3 and Fe^{3+} and Fe^{2+} from the spinel cell of Fe_3O_4 [24, 25]. The presence of Fe_2O_3 in the sample is also confirmed by the stoichiometric calculations which indicate inconsistencies between the total oxygen and the oxygen coming from the silicon layer and magnetite.

Table 1. The content of Fe, Si, N and O identified and determined through ESEM (%) electronic microscopy, without the carbon sublayer.

Crt.	N (Wt%)	O (Wt%)	Si(Wt %)	Fe(Wt %)
P1	0.00	60.45	17.62	21.93
P2	1.97	42.10	22.02	33.91
P3	3.93	60.79	8.56	26.72
P4	2.49	51.40	19.08	24.20
P5	2.90	53.09	26.98	13.02
P6	4.06	53.22	14.05	17.74
P7	1.04	55.87	18.47	22.30
P8	3.50	44.06	20.93	13.76

The fact that besides the C3-C1 there is also C1 in the analysed nanoparticle suspensions explains the gap between the theoretic percents of the constitutive elements and the ones identified practically in the emission spectra of characteristic X rays (tab.1).

The Fe percent may be reused as reference in determining the distribution pattern of the C1 on the Fe_3O_4 surface, supposing that the rising speed of the silicon layer is the same in any point on the surface of a magnetite nanoparticle.

The oxygen percent from the C3 comes from the Fe_3O_4 , C1 cores and the associated water. This makes difficult to use of the emission spectra as elements of quantitative analysis and prediction of C3 synthesis (dimensions, geometric form, the thickness of the C1 layer, etc.) [26, 27, 28].

One notices that the molar ratio $\text{Si}/\text{N}=1:1$ is not observed. This indicates that the $-\text{NH}_2$ groups are distributed regnant on the exterior surface of C3 and C1 (fig.4) and imply other reaction mechanisms for explain -

NH_2 substitution. Supposing that the hypothesis referring to the distribution pattern of $-\text{NH}_2$ is true, it ensues that the specific surface of the synthetised nanostructures is directly proportional with the nitrate content ($-\text{NH}$) determined from the specific X radiation spectra.

Intuitively, one can obtain a relative measure of the variance of the silicon quantity deposited in time, which represents graphically relation 1 with respect to time.

$$\frac{[N][O][Si]}{[Fe]} = f(t) \quad (1)$$

The radiation X spectra of the identified elements are shown in Fig. 4., (we left out the absorbion lines of the carbon used as a material support of the analysed nanoparticles).

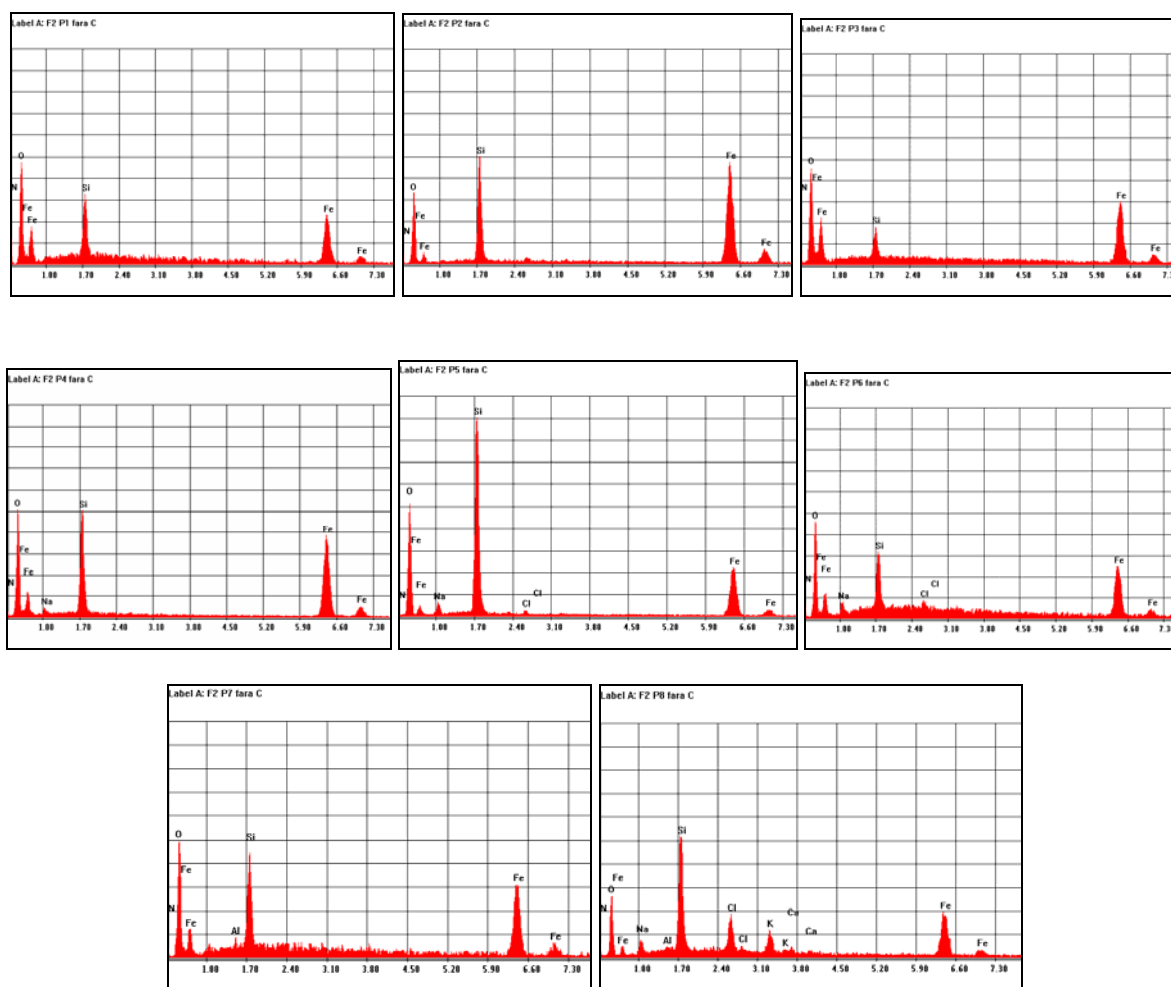


Fig. 4. The XR fluorescence spectra of the investigated samples.

In the chart in Fig.5 one can notice, as expected, that the silicon quantity deposited in time varies linear. The rising speed of the C1 nanolayer on the Fe_3O_4 surface is

given (to a constant which will not be determined in this paper) by relation (2):

$$\frac{\partial d}{\partial (\%Si)} = ct \cdot \frac{3}{4\pi} = A, A = ct. \quad (2)$$

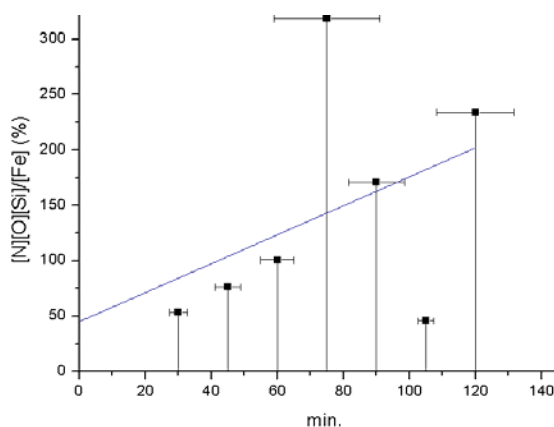
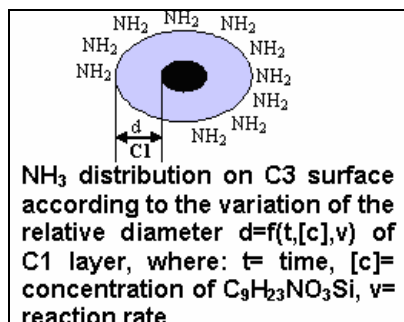


Fig. 5. Data A: - $\frac{[N][O][Si]}{[Fe]}$ experimental points (%) as time function
- Model: $y = (b+cx)(a+x)$, $a = 7.77$, $b = 3.49$, $c = 1.01$

4. Conclusions

The present paper shows a simple and economic way of the controlled synthesis of magnetite nanoparticles coated in C1 and with $-\text{NH}_2$ groups of biochemical interfacing inserted at the cutting line of the silicon layer with the environment. The analysis of the coating speed of the C1 nanolayer permits the thickness control of the silicon layer coated in such a manner as to control the reaction in time according to the necessities. For applications in the field of biochemistry or which require controlled handling of fixed nanostructures, it is recommendable that the C1 layer should be as thin and uniformly distributed as possible.

Magnetite nanoparticles with sizes situated under the limit of super paramagnetic field (30nm) were synthesized and stabilized, in order to disperse them in non-polar solvents.

The synthesized C3 suspension shows high stability from the point of view of the chemical interactions of the

C3-S—S-C3 type bound to take place in the carrying fluid. This recommends the synthesized nanostructures type for the fixing, separation and local and/or global control of the target biostructures.

References

- [1] J. L. Kirschvink, D. S. Jones, B. J. Macfadden, Magnetite biomineralisation and magneto-reception in organisms Ed. Plenum Press N.Y., **1**, p. 43 (1985).
- [2] G. Iacob, O. Rotariu, N. J. C. Strachan, U. Häfeli, Biorheology **41**, 599 (2004).
- [3] S. Chikazumi, Physics of ferromagnetism, 2nd edition, Oxford University Press 1997.
- [4] U. Häfeli, W. Schutt, J. Teller, M. Zborowski, Scientific and Clinical Applications of Magnetic Carriers, 1st edn., Ed. Plenum Press N.Y., 1997.
- [5] J. Smith, H. P. J. Wijn, Ferrites John Wiley and Sons, N.Y., 1959.
- [6] J. F. Yu, U. O. Häfeli, Y. Dong et al., Eur. Cells Mat., 3 Suppl. 2, 16 (2002)
- [7] R. M. Cornell, The Iron Oxides: Structures, Properties, Reactions, Occurrence and Uses, VCH Publishers, Weinheim, 1996.
- [8] H. St. C. O'Neill, A. Navrotsky, Am. Mineral. **68**, 181 (1983).
- [9] M. L. Carpenter, E. K. H. Salje, Am. Mineral., **79**, 1068 (1994).
- [10] U. Häfeli, G. J. Pauer, J. Magn. Magn. Mater. **194**, 76 (1999).
- [11] K. Saatchi, U. O. Häfeli, Dalton Trans **39**, 4439 (2007).
- [12] F. A. Tourinho, R. Franck, R. Massart, R. Perzynsky, Progr. Colloid Polym Sci. **79**, 128 (1989).
- [13] E. Auzâns, D. Zins, M. Maiorov, E. Blûms, R. Massart, Latv. Journ. Phys. and Techn. Sci. **N4**, 29 (1995).
- [14] D. Sellmyer, R. Skomski, Advanced Magnetic Nanostructures, Springer, chapter **3**, 2006.
- [15] R. Massart, IEEE Trans. Magn. **MAG-17**, 1247 (1981).
- [16] F. A. Tourinho, R. Franck, R. Massart, J. Mater. Sci. **25**, 3249 (1990).
- [17] E. Tombácz, A. Majzik, Z. S. Horvát, E. Illés, Rom. Rev. Phys. **58** (3), 281 (2006).
- [18] Y. Sun, L. Duan, Z. Guo, Y. D. Mu, M. Ma, L. Xu, Y. Zhang, N. Gu, J. Magn. Magn. Mater. **285**, 65 (2005).
- [19] C. R. Deltcheff, R. Franck, V. Cabuil, R. Massart, J. Chem. Res. (S), 126 (1987).
- [20] Y. Deng, C. Wang, X. Shen, W. Yang, L. Jin, H. Gao, S. Fu, Chem. Eur. J., **11**, 6006 (2005).
- [21] J. Guo, W. Yang, Y. Deng, C. Wang, S. Fu, small **1**, 737 (2005).
- [22] D. Bojin, F. Miculescu, D. Bunea, M. Miculescu, Scanning electron microscopy and applications, Ed. Agir, Bucharest, 2005.
- [23] V. P. Chalvi, E.N.Lukachina, Neorg. Mater. **1** (2), 260 (1965).

- [24] E. Auzâns, D. Zins, M. M. Maiorov, E. Blûms, R. Massart, *Magn. Hidrodinamika* **36** (1), 78 (1999).
- [25] G. F. Goya, R. F. Pacheco, M. Arruebo, N. Cassinelli, M. R. Ibarra, *J. Magn. Mater.* **316**, 132 (2007).
- [26] R. Rosensweig, Cambridge University Press, Cambridge 61 (1985).
- [27] A. Grants, A. Irbitis, G. Kronkalns, M. Maiorov, *J. Magn. Mater.* **85**, 129 (1990).
- [28] E. Blum, M. M. Maiorov, *Magnetic Fluids*, Walter de Gruyter (Ed.), Berlin, 1997.

*Corresponding author: iordachezamora1978@gmail.com